

Strong $B_{QQ'}^* B_{QQ'} V$ vertices and the radiative decays of $B_{QQ}^* \rightarrow B_{QQ} \gamma$ in the light-cone sum rules

T. M. Aliev^{*}

Physics Department, Middle East Technical University, Ankara 06800, Turkey

T. Barakat[†]

Physics & Astronomy Department, King Saud University, Riyadh 11451, Saudi Arabia

K. Şimşek[‡]

*Department of Physics & Astronomy,
Northwestern University, Evanston, Illinois 60208, USA*

(Dated: January 26, 2021)

Abstract

The strong coupling constants of spin-3/2 to spin-1/2 doubly heavy baryon transitions with light vector mesons are estimated within the light-cone QCD sum rules method. Moreover, using the vector-meson dominance ansatz, the widths of radiative decays $B_{QQ}^* \rightarrow B_{QQ} \gamma$ are calculated. The results for the said decay widths are compared to the predictions of other approaches.

^{*} taliev@metu.edu.tr

[†] tbarakat@ksu.edu.sa

[‡] ksimsek@u.northwestern.edu

I. INTRODUCTION

The quark model is a vital tool for the classification of hadronic states. It predicts the existence of numerous doubly heavy baryons. Among various doubly heavy baryon states, only two, namely Ξ_{cc}^{++} and Ξ_{cc}^+ , have been observed. The first observation of Ξ_{cc}^+ was announced by the SELEX Collaboration in the channels $\Xi_{cc}^+ \rightarrow \Lambda_c^+ K^- \pi^+$ and $p D^+ K^-$ with a mass 3518.7 ± 1.7 MeV [1]. In 2017, the LHCb Collaboration announced an observation of the doubly heavy baryon Ξ_{cc}^{++} in the mass spectrum $\Lambda_c^+ K^- \pi^+ \pi^-$ [2] and confirmed also by measuring another decay channel, $\Xi_{cc}^{++} \rightarrow \Xi_c^+ \pi^+$ [3], with an average mass obtained as $3621.24 \pm 0.65 \pm 0.31$ MeV. The observation of doubly heavy baryon states stimulated new experimental studies in this direction [4, 5].

Theoretical studies on this subject include the study of weak, electromagnetic, and strong decays of doubly heavy baryons. Their weak and strong decays have been comprehensively analyzed within the framework of the light-front QCD, QCD sum rules, and the light-cone sum rules (LCSR) method [6–14]. Their electromagnetic properties and radiative decays have been discussed in [15–18]. The strong couplings of doubly heavy baryons with light mesons within the light-cone sum rules have been studied in [19–23]. These coupling constants are the main parameters for understanding the dynamics of strong decays. The coupling constants of spin-3/2 to spin-1/2 doubly heavy baryons with ρ^+ and K^* have been studied in [20] within the framework of the LCSR method.

The aim of this work is two-fold. First, we extend our previous work [20] to study the vertices $\Xi_{QQ'q}^* \Xi_{QQ'q} \omega$ and $\Omega_{QQ's}^* \Omega_{QQ's} \phi$, where $\Xi_{QQ'q}^*$ ($\Omega_{QQ's}^*$) and $\Xi_{QQ'q}$ ($\Omega_{QQ's}$) denote the spin-3/2 and spin-1/2 doubly heavy baryons, respectively, within the LCSR method and second, using the results for these vertices and assuming the vector-meson dominance (VMD), we estimate the radiative decay widths of $\Xi_{QQq}^* \rightarrow \Xi_{QQq} \gamma$ and $\Omega_{QQs}^* \rightarrow \Omega_{QQs} \gamma$. In all the following discussion, we will denote the spin-3/2 (1/2) doubly heavy baryons by $B_{QQ'}^*$ ($B_{QQ'}$) customarily.

The paper is organized as follows. In Sec. II, first, we derive the LCSR for the coupling constants of the light vector mesons ω and ϕ for the $\Xi_{QQ'q}^* \Xi_{QQ'q} \omega$ and $\Omega_{QQ's}^* \Omega_{QQ's} \phi$ vertices; second, we present the results for the radiative decays $\Xi_{QQq}^* \rightarrow \Xi_{QQq} \gamma$ and $\Omega_{QQs}^* \rightarrow \Omega_{QQs} \gamma$ by assuming the VMD. Sec. III contains the numerical analysis of the obtained sum rules for

the strong coupling constants and radiative decays. A summary and conclusion are presented in Sec. IV.

II. THE $B_{QQ'q}^* B_{QQ'q} V$ VERTICES IN THE LIGHT-CONE SUM RULES

By using the Lorentz invariance, the vertices $B_{QQ'}^* B_{QQ'} V$, where $V = \rho^0$, ω , or ϕ and $B^{(*)} = \Xi^{(*)}$ or $\Omega^{(*)}$, are parametrized in terms of three coupling constants, g_1 , g_2 , and g_3 , as follows [24]:

$$\begin{aligned} \langle V(q) B_{QQ'}^*(p_2) | B_{QQ'}(p_1) \rangle = & \bar{u}_\alpha(p_2) [g_1 (\varepsilon^{*\alpha} \not{q} - q^\alpha \not{\varepsilon}^*) \gamma_5 + g_2 (P \cdot q \varepsilon^{*\alpha} - P \cdot \varepsilon^* q^\alpha) \gamma_5 \\ & + g_3 (q \cdot \varepsilon^* q^\alpha - q^2 \varepsilon^{*\alpha}) \gamma_5] u(p_1) \end{aligned} \quad (1)$$

where $u_\alpha(p_2)$ is the Rarita-Schwinger spinor for a spin-3/2 baryon, ε_α is the 4-polarization vector of the light vector meson V , $P = (p_1 + p_2)/2$, and $q = p_1 - p_2$. In the rest of the text, we denote $p_2 = p$ and $p_1 = p + q$.

For the determination of the said three coupling constants, g_1 , g_2 , and g_3 , within the LCSR, we introduce the following correlation function:

$$\Pi_\mu(p, q) = i \int d^4x e^{ipx} \langle V(q) | T \{ \eta_\mu(x) \bar{\eta}(0) \} | 0 \rangle \quad (2)$$

where $V(q)$ is a light vector meson (ρ^0 , ω , or ϕ) with 4-momentum q_μ , and η_μ and η are the interpolating currents for the spin-3/2 and spin-1/2 baryons, respectively. The most general form of the interpolating currents of spin-3/2 and spin-1/2 baryons doubly heavy baryons are

$$\eta_\mu = N \epsilon^{abc} \{ (q^{aT} C \gamma_\mu Q^b) Q'^c + (q^{aT} C \gamma_\mu Q'^b) Q^c + (Q^{aT} C \gamma_\mu Q^b) q^c \} \quad (3)$$

$$\eta^{(S)} = \frac{1}{\sqrt{2}} \epsilon^{abc} \sum_{i=1}^2 [(Q^{aT} A_1^i q^b) A_2^i Q'^c + (Q \leftrightarrow Q')] \quad (4)$$

$$\eta^{(A)} = \frac{1}{\sqrt{6}} \epsilon^{abc} \sum_{i=1}^2 [2(Q^a A_1^i Q'^b) A_2^i q^c + (Q^{aT} A_1^i Q'^c) - Q'^{aT} A_1^i q^b] A_2^i Q^c \quad (5)$$

where T is the transpose, $N = \sqrt{1/3}$ ($\sqrt{2/3}$) for identical (distinct) heavy quarks, $A_1^1 = C$, $A_2^1 = \gamma_5$, $A_1^2 = C\gamma_5$, and $A_2^2 = \beta I$, the superscripts S and A denote symmetric and antisymmetric interpolating currents with respect to the interchange of heavy quarks, and β is the arbitrary parameter, for which $\beta = -1$ corresponds to the case of the Ioffe current.

The LCSR for the coupling constants, g_1 , g_2 , and g_3 , is obtained by calculating the correlation function in two different regions: First, in terms of hadrons, and second, in the deep Euclidean domain by using operator product expansion (OPE). In terms of hadrons, the correlation function is obtained by inserting a complete set of intermediate hadronic states carrying the same quantum numbers as the interpolating currents η_μ and η and using the quark-hadron duality. After isolating the ground state contribution, we get

$$\begin{aligned} \Pi_\mu(p, q) = & \frac{\lambda_1 \lambda_2}{(m_1^2 - p^2)[m_2^2 - (p + q)^2]} [-g_1(m_1 + m_2) \not{\epsilon}^* \not{p} \gamma_5 q_\mu + g_2 \not{q} \not{p} \gamma_5 p \cdot \varepsilon^* q_\mu + g_3 q^2 \not{q} \not{p} \gamma_5 \varepsilon_\mu^* \\ & + \text{other structures}] \end{aligned} \quad (6)$$

Here, ε^μ is the 4-polarization vector of the light vector meson. In the derivation of Eq. (6), the following definitions have been used:

$$\langle 0 | \eta | B_{QQ'}(p) \rangle = \lambda_1 u(p, s) \quad (7)$$

$$\langle 0 | \eta_\mu | B_{QQ'}^*(p) \rangle = \lambda_2 u_\mu(p, s) \quad (8)$$

where λ_1 (m_1) and λ_2 (m_2) are the residues (masses) of the spin-3/2 and spin-1/2 states, respectively. The summation over spin-1/2 and spin-3/2 baryons is performed by using the corresponding completeness relations:

$$\sum_s u(p, s) \bar{u}(p, s) = \not{p} + m \quad (9)$$

$$\sum_s u_\mu(p, s) \bar{u}_\nu(p, s) = -(\not{p} + m) \left[g_{\mu\nu} - \frac{1}{3} \gamma_\mu \gamma_\nu - \frac{2}{3} \frac{p_\mu p_\nu}{m^2} + \frac{1}{3} \frac{p_\mu \gamma_\nu - p_\nu \gamma_\mu}{m} \right] \quad (10)$$

At this point, we would like to make the following remarks:

- (a) The current η_μ couples also to spin-1/2 baryons, $B(p)$, with the corresponding matrix element

$$\langle 0 | \eta_\mu | B^-(p) \rangle = A \left(\gamma_\mu - \frac{4}{m} p_\mu \right) u(p, s) \quad (11)$$

Hence, the structures containing γ_μ or p_μ include contributions from the 1/2 states. From Eq. (10), it follows that only structure proportional to $g_{\mu\nu}$ is free of 1/2 state contributions.

- (b) Not all Lorentz structures are independent. This problem can be solved by using the specific order of Dirac matrices. In the present work, we specify the desired order of Dirac matrices to be in the form $\gamma_\mu \not{\epsilon} \not{q} \not{p} \gamma_5$.

We choose the Lorentz structures $\not{\epsilon} \not{p} \gamma_5 q_\mu$, $\not{q} \not{p} \gamma_5 \not{q} q_\mu$, and $\not{q} \not{p} \gamma_5 \epsilon_\mu$ for the determination of the coupling constants g_1 , g_2 , and g_3 which are free from $1/2$ contamination and which also yield better stability in the numerical analysis.

The correlation function in the deep Euclidean domain, $p^2 \ll 0$ and $(p+q)^2 \ll 0$, can be calculated by using OPE near the light cone. The ample details of calculations are presented in [20] and for this reason, we do not repeat them here.

In the final step, performing a double Borel transformation over the variables $-p^2$ and $-(p+q)^2$, choosing the coefficients of the same Lorentz structures in both representations and matching them, and using the quark-hadron duality ansatz, we get the desired sum rules for these strong coupling constants:

$$g_1 = -\frac{1}{\lambda_1 \lambda_2 (m_1 + m_2)} e^{m_1^2/M_1^2 + m_2^2/M_2^2} \Pi_1^{(S)} \quad (12)$$

$$g_2 = \frac{1}{\lambda_1 \lambda_2} e^{m_1^2/M_1^2 + m_2^2/M_2^2} \Pi_2^{(S)} \quad (13)$$

$$g_3 = \frac{1}{\lambda_1 \lambda_2} e^{m_1^2/M_1^2 + m_2^2/M_2^2} \Pi_3^{(S)} \quad (14)$$

While one discovers that all the terms vanish for the antisymmetric case, the explicit expressions of $\Pi_i^{(S)}$ can be found in [20].

At the end of this section, we derive the corresponding coupling constants for the vertices $B_{QQ}^* B_{QQ} \gamma$ by using the VMD ansatz. The VMD implies that the $B_{QQ}^* B_{QQ} \gamma$ vertex can be obtained from $B_{QQ}^* B_{QQ} V$ by converting the corresponding vector meson to a photon. From the gauge invariance, the $B_{QQ}^* B_{QQ} \gamma$ vertex is parametrized similarly to the $B_{QQ}^* B_{QQ} V$ vertex as follows:

$$\begin{aligned} \langle \gamma(q) B_{QQ}^*(p_2) | B_{QQ}(p_1) \rangle = & \bar{u}^\alpha(p_2) [g_1^\gamma (\epsilon_\alpha^{*\gamma} \not{q} - q_\alpha \not{\epsilon}^{*\gamma}) \gamma_5 + g_2^\gamma (P \cdot q \epsilon_\alpha^{*\gamma} - P \cdot \epsilon^{*\gamma} q_\alpha) \gamma_5 \\ & + g_3^\gamma (q \cdot \epsilon^{*\gamma} q^\alpha - q^2 \epsilon_\alpha^{*\gamma}) \gamma_5] u(p_1) \end{aligned} \quad (15)$$

Obviously, the last term for real photons is equal to zero. To obtain the vertex $B_{QQ}^* B_{QQ} \gamma$ from the $B_{QQ}^* B_{QQ} V$, it is necessary to make the replacement

$$\epsilon_\mu \rightarrow e \sum_{V=\rho^0, \omega, \phi} e_q \frac{f_V}{m_V} \epsilon_\mu^\gamma \quad (16)$$

and go from $q^2 = m_V^2$ to $q^2 = 0$. Let's check this statement.

The radiative decays $B_{QQ}^* \rightarrow B_{QQ}\gamma$ can be described by the following Lagrangian:

$$\mathcal{L} = iee_Q \bar{Q} \gamma_\mu Q A^\mu + iee_q \bar{q} \gamma_\mu q A^\mu \quad (17)$$

From this Lagrangian, one can obtain the decay amplitudes with the incorporation of the VMD, i.e.

$$\begin{aligned} \langle \gamma(q) B_{QQq}^*(p) | \mathcal{L} | B_{QQq}(p+q) \rangle &= iee_q \varepsilon^{*\gamma\mu} \langle B_{QQq}^*(p) | \bar{q} \gamma_\mu q | B_{QQq}(p+q) \rangle \\ &= ee_s \varepsilon^{*\gamma\mu} \frac{\varepsilon_\mu}{q^2 - m_\phi^2} \langle \phi(q) B_{QQs}^*(p) | B_{QQs}(p+q) \rangle \\ &\quad + ee_q \varepsilon^{*\gamma\mu} \frac{\varepsilon_\mu}{q^2 - m_\rho^2} \langle \rho(q) B_{QQq}^*(p) | B_{QQq}(p+q) \rangle \\ &\quad + ee_q \varepsilon^{*\gamma\mu} \frac{\varepsilon_\mu}{q^2 - m_\omega^2} \langle \omega(q) B_{QQq}^*(p) | B_{QQq}(p+q) \rangle \end{aligned} \quad (18)$$

At the point $q^2 = 0$, (real photon case), this expression is simplified and we have

$$\begin{aligned} \langle \gamma(q) B_{QQq}^*(p) | \mathcal{L} | B_{QQq}(p+q) \rangle &= ee_s \varepsilon^{*\gamma} \cdot \varepsilon \frac{f_\phi}{m_\phi} \langle \phi(q) B_{QQs}^*(p) | B_{QQs}(p+q) \rangle \\ &\quad + ee_q \varepsilon^{*\gamma} \cdot \varepsilon \frac{f_\rho}{m_\rho} \langle \rho(q) B_{QQq}^*(p) | B_{QQq}(p+q) \rangle \\ &\quad + ee_q \varepsilon^{*\gamma} \cdot \varepsilon \frac{f_\omega}{m_\omega} \langle \omega(q) B_{QQq}^*(p) | B_{QQq}(p+q) \rangle \end{aligned} \quad (19)$$

From Eqs. (1) and (16), for $B_{QQq}^* B_{QQq} \gamma$ vertex, we get

$$\begin{aligned} \langle \gamma(q) B_{QQq}^*(p) | \mathcal{L} | B_{QQq}(p+q) \rangle &= \sum_{V=\rho,\omega,\phi} ee_q \frac{f_V}{m_V} \bar{u}_\alpha(p) [g_1(-q_\mu \not{\varepsilon}^{*\gamma} + \varepsilon_\mu^{*\gamma} \not{q}) \\ &\quad - g_2(P \cdot \varepsilon^{*\gamma} q_\mu - P \cdot q \varepsilon_\mu^{*\gamma})] \gamma_5 u(p+q) \end{aligned} \quad (20)$$

Comparing Eqs. (1) and (20), we obtain the relation among the couplings $B_{QQq}^* B_{QQq} V$ and $B_{QQq}^* B_{QQq} \gamma$

$$g_i^\gamma = \begin{cases} e_s \frac{f_\phi}{m_\phi} g_i^\phi & \text{for } \Omega_{QQs}^* \rightarrow \Omega_{QQs} \gamma \\ e_u \left(\frac{f_\rho}{m_\rho} g_i^\rho + \frac{f_\omega}{m_\omega} g_i^\omega \right) & \text{for } \Xi_{QQu}^* \rightarrow \Xi_{QQu} \gamma \\ e_d \left(-\frac{f_\rho}{m_\rho} g_i^\rho + \frac{f_\omega}{m_\omega} g_i^\omega \right) & \text{for } \Xi_{QQd}^* \rightarrow \Xi_{QQd} \gamma \end{cases} \quad (21)$$

for $i = 1, 2$. Here, we would like to make two remarks. First, we assume that couplings do not change considerably when we go from $q^2 = m_V^2$ to $q^2 = 0$. The second remark is

related to the fact that, in principle, heavy vector meson resonances can also contribute. These contributions are neglected since in the heavy quark limit their contributions are proportional to $m_{\text{heavy meson}}^{-3/2}$.

In the numerical calculations for f_ρ , f_ω , and f_ϕ , we have used the prediction of the sum rules $f_\rho = 205$ MeV, $f_\omega = 185$ MeV, and $f_\phi = 215$ MeV [25].

In this work, instead of the formfactors g_1^γ and g_2^γ , we will use the magnetic dipole and electric quadrupole formfactors, G_M and G_E , respectively, which are more convenient from an experimental point of view. The relation among these formfactors at the $q^2 = 0$ point are

$$G_M = (3m_1 + m_2) \frac{m_2}{3m_1} g_1^\gamma + (m_1 - m_2) m_2 \frac{g_2^\gamma}{3} \quad (22)$$

$$G_E = (m_1 - m_2) \frac{m_2}{3m_1} (g_1^\gamma + m_1 g_2^\gamma) \quad (23)$$

Using these relations, it is straightforward to calculate the decay widths of $B_{QQ}^* B_{QQ} \gamma$ decay. The result is

$$\Gamma = \frac{3\alpha}{4} \frac{k_\gamma^3}{m_2^2} (3G_E^2 + G_M^2) \quad (24)$$

where α is the fine structure coupling and $k_\gamma = (m_1^2 - m_2^2)/2m_1$ is the photon energy.

III. NUMERICAL ANALYSIS

In this section, we perform the numerical analysis of the LCSR for the coupling constants g_1 and g_2 obtained in the previous section for the $\Xi_{QQ'}^* \Xi_{QQ'} \omega$ and $\Omega_{QQ'}^* \Omega_{QQ'} \phi$ vertices by using Package X [26].

The LCSR involves various input parameters, such as the quark masses, the masses and residues of doubly heavy baryons, and the decay constants of the light vector mesons, ω and ϕ . These parameters are collected in Table I.

Table I: Part of the input parameters. The masses and decay constants are at $\mu = 1$ GeV and in units of GeV.

| Parameter | Value | Parameter | Value | Parameter | Value | Parameter | Value | Parameter | Value | Parameter | Value |
|-----------|-------|--------------|-------|---------------------|-------------|---------------------------|-----------|-------------------|-------------|-------------------------|-----------|
| m_u | 0 | m_ω | 0.783 | $m_{\Xi_{cc}^*}$ | 3.692 [25] | $\lambda_{\Xi_{cc}^*}$ | 0.12 [27] | $m_{\Xi_{cc}}$ | 3.610 [25] | $\lambda_{\Xi_{cc}}$ | 0.16 [28] |
| m_d | 0 | f_ω | 0.187 | $m_{\Xi_{bb}^*}$ | 10.178 [25] | $\lambda_{\Xi_{cc}^*}$ | 0.22 [27] | $m_{\Xi_{bb}}$ | 10.143 [25] | $\lambda_{\Xi_{bb}}$ | 0.44 [28] |
| m_s | 0.137 | f_ω^T | 0.151 | $m_{\Xi_{bc}^*}$ | 6.985 [25] | $\lambda_{\Xi_{cc}^*}$ | 0.15 [27] | $m_{\Xi_{bc}}$ | 6.943 [25] | $\lambda_{\Xi_{bc}}$ | 0.28 [28] |
| m_c | 1.4 | m_ϕ | 1.019 | $m_{\Omega_{cc}^*}$ | 3.822 [25] | $\lambda_{\Omega_{cc}^*}$ | 0.14 [27] | $m_{\Omega_{cc}}$ | 3.738 [25] | $\lambda_{\Omega_{cc}}$ | 0.18 [28] |
| m_b | 4.8 | f_ϕ | 0.215 | $m_{\Omega_{bb}^*}$ | 10.308 [25] | $\lambda_{\Omega_{cc}^*}$ | 0.25 [27] | $m_{\Omega_{bb}}$ | 10.273 [25] | $\lambda_{\Omega_{bb}}$ | 0.45 [28] |
| | | f_ϕ^T | 0.186 | $m_{\Omega_{bc}^*}$ | 7.059 [25] | $\lambda_{\Omega_{cc}^*}$ | 0.17 [27] | $m_{\Omega_{bc}}$ | 6.998 [25] | $\lambda_{\Omega_{bc}}$ | 0.29 [28] |

The main nonperturbative input parameters of the LCSR are the vector meson distribution amplitudes (DAs). The explicit expressions of the vector meson DAs are given in [20] and references therein. The parameters that appear in the light vector meson DAs for ω and ϕ are presented in Table II.

Table II: Vector meson DA parameters for ω and ϕ at $\mu = 1$ GeV [29–34]. The accuracy of these parameters are 30–50%.

| Parameter | ω | ϕ | Parameter | ω | ϕ |
|-------------------------------|----------|--------|------------------------------|----------|--------|
| a_1^\parallel | 0 | 0 | κ_3^\perp | 0 | 0 |
| a_1^\perp | 0 | 0 | ω_3^\perp | 0.55 | 0.20 |
| a_2^\parallel | 0.15 | 0.18 | λ_3^\perp | 0 | 0 |
| a_2^\perp | 0.14 | 0.14 | ζ_4^\parallel | 0.07 | 0 |
| ζ_3^\parallel | 0.030 | 0.024 | $\tilde{\omega}_4^\parallel$ | −0.03 | −0.02 |
| $\tilde{\lambda}_3^\parallel$ | 0 | 0 | ζ_4^\perp | −0.03 | −0.01 |
| $\tilde{\omega}_3^\parallel$ | −0.09 | −0.045 | $\tilde{\zeta}_4^\perp$ | −0.08 | −0.03 |
| κ_3^\parallel | 0 | 0 | κ_4^\parallel | 0 | 0 |
| ω_3^\parallel | 0.15 | 0.09 | κ_4^\perp | 0 | 0 |
| λ_3^\parallel | 0 | 0 | | | |

The LCSR for the strong coupling constants g_1 and g_2 involves three auxiliary parameters, namely the Borel mass parameter, M^2 , the continuum threshold s_0 , and the parameter β , in the expression of the interpolating current. Hence, we need to find the working regions of

these parameters where the results for the coupling constants g_1 and g_2 practically exhibit insensitivity to the variation of these parameters. The lower bound of M^2 is determined by requiring the contributions of higher twist terms considerably small than the leading twist one (say than 15%). The upper bound of M^2 can be found by requiring that the continuum contribution to the sum rules should be less than 25% of the total result. The value of continuum threshold s_0 is obtained by demanding that the two-point sum rules reproduce the mass of doubly heavy baryons with 10% accuracy. After performing the numerical analysis, we obtained the working regions for M^2 and s_0 as displayed in Table III.

Table III: The working regions of the Borel mass parameter and the central value of the continuum threshold.

| Transition | M^2 (GeV ²) | s_0 (GeV ²) |
|---|---------------------------|---------------------------|
| $\Xi_{cc}^* \rightarrow \Xi_{cc}\omega$ | $3 \leq M^2 \leq 4.5$ | 18 |
| $\Xi_{bb}^* \rightarrow \Xi_{bb}\omega$ | $8 \leq M^2 \leq 12$ | 110 |
| $\Xi_{bc}^* \rightarrow \Xi_{bc}\omega$ | $6 \leq M^2 \leq 8$ | 60 |
| $\Omega_{cc}^* \rightarrow \Omega_{cc}\phi$ | $3 \leq M^2 \leq 5$ | 18 |
| $\Omega_{bb}^* \rightarrow \Omega_{bb}\phi$ | $8 \leq M^2 \leq 13$ | 110 |
| $\Omega_{bc}^* \rightarrow \Omega_{bc}\phi$ | $6 \leq M^2 \leq 9$ | 60 |

Finally, we note that the value of the $\Xi_{QQ}^* \rightarrow \Xi_{QQ}\rho^0$ couplings can be obtained from the results of [20] via the isospin symmetry.

As an illustration, we present the dependence of the coupling constants g_1 , g_2 , and g_3 on $\cos\theta$ for the transition $\Xi_{cc}^* \rightarrow \Xi_{cc}\omega$, where θ is defined via $\beta = \tan\theta$ and on the Borel mass parameter, M^2 in Figs. 1–6. We summarized our results in Table IV. The corresponding values for the case of the Ioffe current, for which $\beta = -1$, are also presented. One can see that in Figs. 1–3, the value of the coupling constant practically does not change for the values of $|\cos\theta|$ between 0.5 and 0.8, hence we determine the working region of β accordingly. The errors in Table IV reflect the uncertainties in the aforementioned input parameters. From this table, it follows that in the case of a general current, the values of the coupling constants are comparable to those in the case of the Ioffe current.

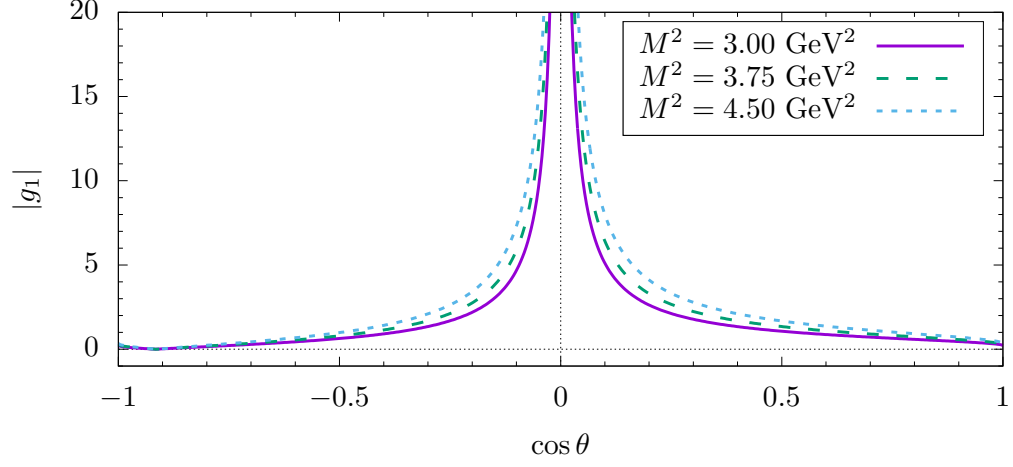


Figure 1: The dependence of the modulus of the coupling constant g_1 for $\Xi_{cc}^* \rightarrow \Xi_{cc}\omega$ on $\cos \theta$ at the shown values of M^2 with $s_0 = 18 \text{ GeV}^2$.

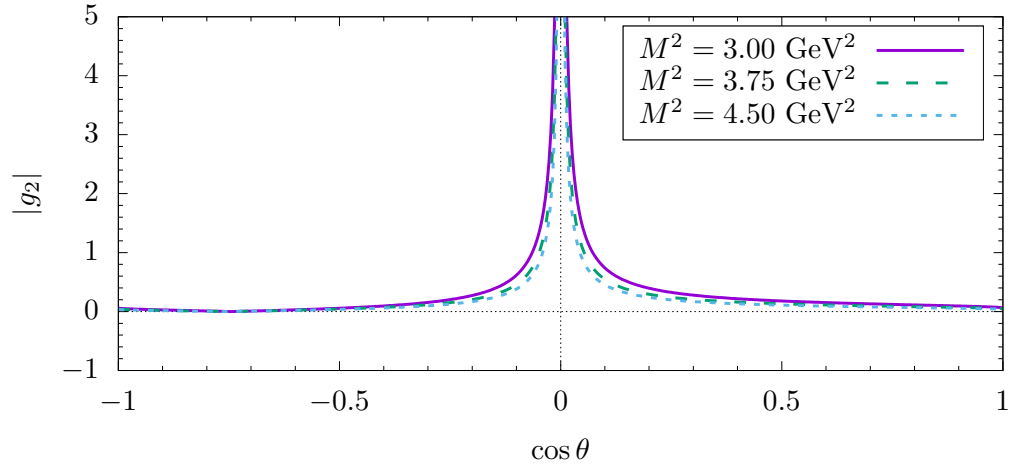


Figure 2: The same as Fig. 1 but for g_2 .

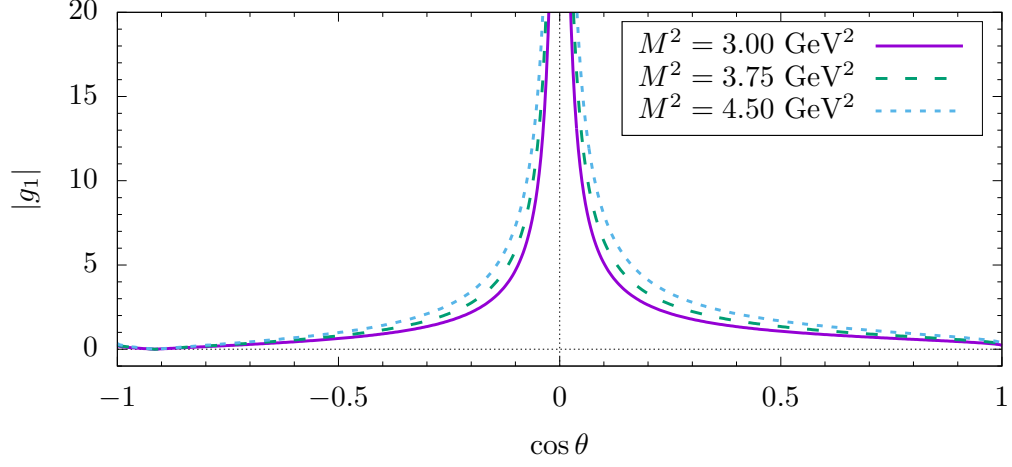


Figure 3: The same as Fig. 1 but for g_3 .

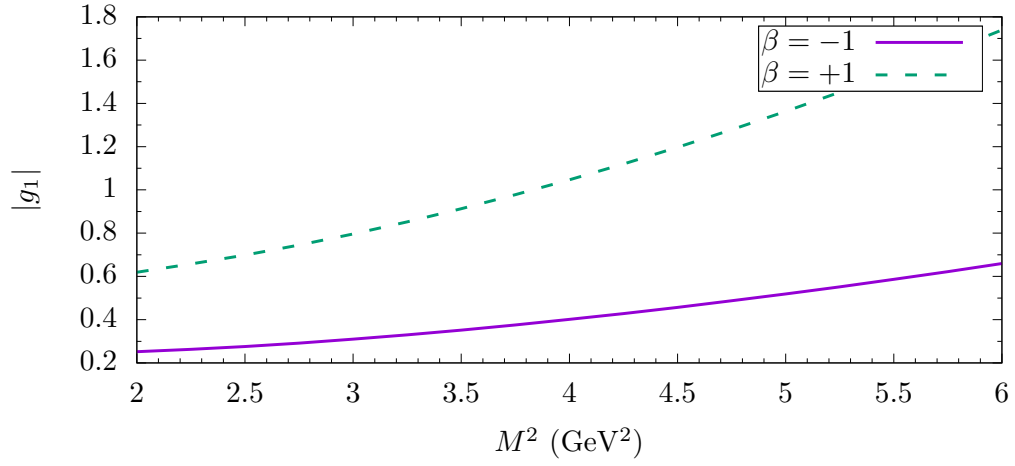


Figure 4: The dependence of the modulus of the coupling constant g_1 for $\Xi_{cc}^* \rightarrow \Xi_{cc}\omega$ on M^2 at the shown values of β with $s_0 = 18 \text{ GeV}^2$.

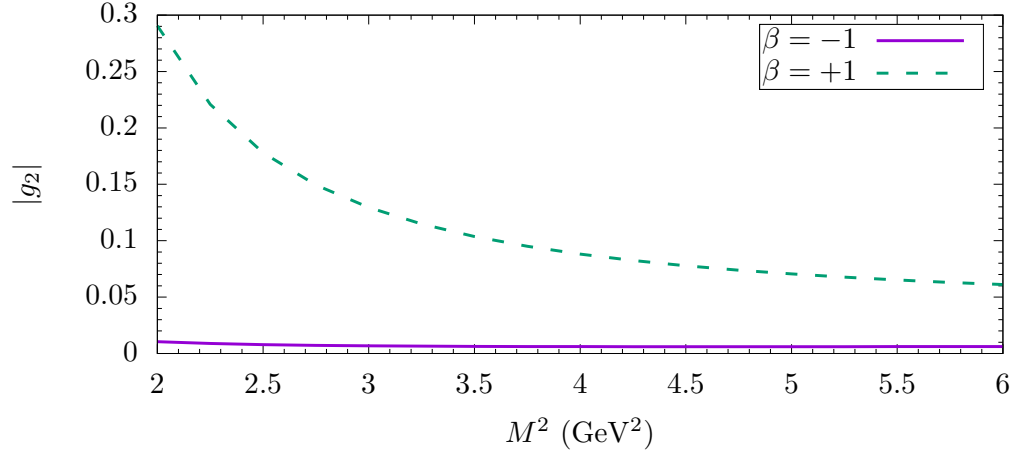


Figure 5: The same as Fig. 4 but for g_2 .

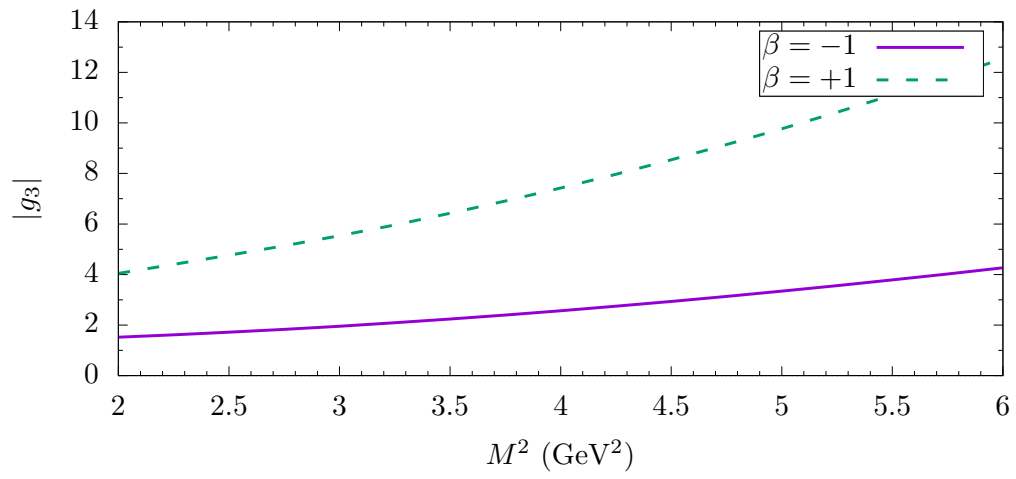


Figure 6: The same as Fig. 4 but for g_3 .

Table IV: The obtained values of the moduli of the coupling constants g_1 , g_2 , and g_3 for the aforementioned transitions accompanied by a light vector meson.

| Case of the general current | | | | Case of the Ioffe current | | |
|---|-----------------|-----------------|------------------|---------------------------|-----------------|------------------|
| Transition | $ g_1 $ | $ g_2 $ | $ g_3 $ | $ g_1 $ | $ g_2 $ | $ g_3 $ |
| $\Xi_{cc}^* \rightarrow \Xi_{cc}\rho^0$ | 1.13 ± 0.25 | 0.11 ± 0.03 | 7.81 ± 1.83 | 0.99 ± 0.22 | 0.10 ± 0.02 | 6.92 ± 1.62 |
| $\Xi_{bb}^* \rightarrow \Xi_{bb}\rho^0$ | 0.76 ± 0.23 | 0.03 ± 0.00 | 15.19 ± 4.64 | 0.67 ± 0.20 | 0.02 ± 0.00 | 13.45 ± 4.11 |
| $\Xi_{bc}^* \rightarrow \Xi_{bc}\rho^0$ | 1.06 ± 0.20 | 0.05 ± 0.01 | 14.44 ± 2.84 | 0.94 ± 0.18 | 0.05 ± 0.01 | 12.79 ± 2.51 |
| $\Xi_{cc}^* \rightarrow \Xi_{cc}\omega$ | 1.02 ± 0.23 | 0.10 ± 0.02 | 7.10 ± 1.68 | 0.90 ± 0.20 | 0.09 ± 0.02 | 6.29 ± 1.49 |
| $\Xi_{bb}^* \rightarrow \Xi_{bb}\omega$ | 0.69 ± 0.21 | 0.03 ± 0.00 | 13.82 ± 4.25 | 0.61 ± 0.19 | 0.02 ± 0.00 | 12.24 ± 3.77 |
| $\Xi_{bc}^* \rightarrow \Xi_{bc}\omega$ | 0.97 ± 0.19 | 0.05 ± 0.01 | 13.14 ± 2.60 | 0.86 ± 0.17 | 0.05 ± 0.01 | 11.64 ± 2.31 |
| $\Omega_{cc}^* \rightarrow \Omega_{cc}\phi$ | 1.50 ± 0.32 | 0.50 ± 0.14 | 9.79 ± 2.50 | 1.32 ± 0.28 | 0.45 ± 0.13 | 8.64 ± 2.22 |
| $\Omega_{bb}^* \rightarrow \Omega_{bb}\phi$ | 1.22 ± 0.35 | 0.15 ± 0.03 | 23.90 ± 7.19 | 1.08 ± 0.31 | 0.14 ± 0.03 | 21.15 ± 6.38 |
| $\Omega_{bc}^* \rightarrow \Omega_{bc}\phi$ | 1.47 ± 0.29 | 0.25 ± 0.04 | 19.26 ± 4.13 | 1.30 ± 0.26 | 0.22 ± 0.03 | 17.03 ± 3.66 |

Now using the obtained results for g_1 and g_2 , we can estimate g_i^γ and hence G_M and G_E . The results for G_M and G_E are collected in Table V.

Table V: The electric quadrupole and magnetic dipole formfactors for the shown transitions.

| Transition | $ G_E $ | $ G_M $ |
|--|-----------------|-----------------|
| $\Xi_{cc}^{*++} \rightarrow \Xi_{cc}^{++}\gamma$ | 0.00 ± 0.00 | 1.78 ± 0.40 |
| $\Xi_{cc}^{*+} \rightarrow \Xi_{cc}^{+}\gamma$ | 0.00 ± 0.00 | 0.11 ± 0.02 |
| $\Xi_{bb}^{*0} \rightarrow \Xi_{bb}^0\gamma$ | 0.00 ± 0.00 | 3.41 ± 1.03 |
| $\Xi_{bb}^{*-} \rightarrow \Xi_{bb}^{-}\gamma$ | 0.00 ± 0.00 | 0.22 ± 0.06 |
| $\Omega_{cc}^{*+} \rightarrow \Omega_{cc}^{+}\gamma$ | 0.00 ± 0.00 | 0.52 ± 0.11 |
| $\Omega_{bb}^{*-} \rightarrow \Omega_{bb}^{-}\gamma$ | 0.00 ± 0.00 | 1.18 ± 0.34 |

Using Eq. (24) and the values of G_M and G_E for the decay widths of these transitions, it is straightforward to find the values of the corresponding decay widths. From Eq. (24), one can see that the decay width is very sensitive to the mass difference of the considered baryons, $\Delta m = m_1 - m_2$. Therefore, a tiny change in the mass difference leads to a significant change in the decay width. To see this, as an example, we present the decay widths for the transition

$\Omega_{ccs}^* \rightarrow \Omega_{ccs}\gamma$ by using the different mass differences obtained in various approaches. The results are presented in Table VI.

Table VI: The decay width of the transition $\Omega_{ccs}^* \rightarrow \Omega_{ccs}\gamma$ for different mass splittings.

| Δm [MeV] | 57 [35] | 61 [36] | 73 [37] | 84 [25] | 94 [7, 38, 39] | 100 [17] |
|------------------|---------|---------|---------|---------|----------------|----------|
| Γ [keV] | 0.07 | 0.09 | 0.15 | 0.23 | 0.33 | 0.40 |

In our numerical calculations, for the masses of spin-1/2 and spin-3/2 states, we have used the results of [25] (see Table I) because the results are practically free from errors. Our final results on the decay widths are collected in Table VII. For completeness, we also presented the results for corresponding decay widths obtained within different approaches. From the comparison of decay widths, we see that our result only for the $\Omega_{cc}^* \rightarrow \Omega_{cc}\gamma$ decay is close to the prediction of the lattice theory and considerably different from the ones in other existing approaches. One possible source of these discrepancies may be that, for doubly heavy baryon systems, the VMD ansatz may work not so quite well. In order to see how the VMD works for doubly heavy baryon systems, it would be useful to calculate G_M and G_E directly, i.e. without using the VMD ansatz. This work is in progress.

Table VII: The widths of the shown radiative decays in units of keV.

| Transition | Our work | Chiral quark model [7] | Three-quark model [38] | Chiral perturbation theory [17] | Lattice QCD [18] |
|--|-----------------------------------|------------------------|------------------------|---------------------------------|-----------------------|
| $\Xi_{cc}^{*++} \rightarrow \Xi_{cc}^{++}\gamma$ | $(71.33 \pm 3.56) \times 10^{-2}$ | 16.7 | 23.5 | 22 | 7.77×10^{-2} |
| $\Xi_{cc}^{*+} \rightarrow \Xi_{cc}^{+}\gamma$ | $(0.29 \pm 0.01) \times 10^{-2}$ | 14.6 | 28.8 | 9.57 | 9.72×10^{-2} |
| $\Omega_{cc}^* \rightarrow \Omega_{cc}\gamma$ | $(6.08 \pm 0.28) \times 10^{-2}$ | 6.93 | 2.11 | 9.45 | 8.47×10^{-2} |
| $\Xi_{bb}^{*0} \rightarrow \Xi_{bb}^0\gamma$ | $(2.64 \pm 0.24) \times 10^{-2}$ | 1.19 | 0.31 | — | — |
| $\Xi_{bb}^{*-} \rightarrow \Xi_{bb}^{-}\gamma$ | $(0.01 \pm 0.00) \times 10^{-2}$ | 0.24 | 0.06 | — | — |
| $\Omega_{bb}^* \rightarrow \Omega_{bb}\gamma$ | $(0.31 \pm 0.03) \times 10^{-2}$ | 0.08 | 0.02 | — | — |

IV. CONCLUSION

In the present work, first, we estimated the strong coupling constants of $B_{QQ'}^* B_{QQ'} V$ vertices within the framework of the LCSR method. Then, assuming the VMD model, we calculated the magnetic dipole and electric quadrupole formfactors, G_M and G_E , respectively,

at the point $Q^2 = 0$. Using the results for G_M and G_E , we obtained the decay widths of the radiative decays $B_{QQ}^* \rightarrow B_{QQ}\gamma$. Our result for the decay widths of $\Omega_{cc}^* \rightarrow \Omega_{cc}\gamma$ is in good agreement with the lattice result and considerably different from the prediction of other channels in various approaches. Our predictions on the strong coupling constants for the radiative $B_{QQ}^* B_{QQ} V$ vertices, as well as the decay widths, can be checked at LHCb experiments in the future.

-
- [1] M. Mattson *et al.* (SELEX Collaboration), [Phys. Rev. Lett. **89**, 112001 \(2002\)](#).
 - [2] R. Aaij *et al.* (LHCb Collaboration), [Phys. Rev. Lett. **119**, 112001 \(2017\)](#).
 - [3] R. Aaij *et al.* (LHCb Collaboration), [Phys. Rev. Lett. **121**, 162002 \(2018\)](#).
 - [4] R. Aaij *et al.* (LHCb Collaboration), [J. High Energy Phys. **2019**, 124 \(2019\)](#).
 - [5] R. Aaij *et al.* (LHCb Collaboration), [J. High Energy Phys. **2020**, 49 \(2020\)](#).
 - [6] W. Wang, Z. P. Xing, and J. Xu, [Eur. Phys. J. C **77**, 800 \(2017\)](#).
 - [7] L. Y. Xiao, K. L. Wang, Q. F. Lü, X. H. Zhong, and S. L. Zhu, [Phys. Rev. D **96**, 094005 \(2017\)](#).
 - [8] W. Wang, F. S. Yu, and Z. X. Zhao, [Eur. Phys. J. C **77**, 781 \(2017\)](#).
 - [9] H. Y. Cheng and Y. L. Shi, [Phys. Rev. D **98**, 113005 \(2018\)](#).
 - [10] Y. J. Shi, W. Wang, Y. Xing, and J. Xu, [Eur. Phys. J. C **78**, 56 \(2018\)](#).
 - [11] Z. X. Zhao, [Eur. Phys. J. C **78**, 756 \(2018\)](#).
 - [12] Y. J. Shi, W. Wang, and Z. X. Zhao, [Eur. Phys. J. C **80**, 568 \(2020\)](#).
 - [13] Y. J. Shi and Z. X. Zhao, [Eur. Phys. J. C **79**, 501 \(2019\)](#).
 - [14] X. H. Hu and Y. J. Shi, [Eur. Phys. J. C **80**, 56 \(2020\)](#).
 - [15] H. S. Li, L. Meng, Z. W. Liu, and S. L. Zhu, [Phys. Rev. D **96**, 076011 \(2017\)](#).
 - [16] L. Meng, H. S. Li, Z. W. Liu, and S. L. Zhu, [Eur. Phys. J. C **77**, 869 \(2017\)](#).
 - [17] H. S. Li, L. Meng, Z. W. Liu, and S. L. Zhu, [Phys. Lett. B **777**, 169 \(2018\)](#).
 - [18] H. Bahtiyar, K. U. Can, G. Erkol, M. Oka, and T. T. Takahashi, [Phys. Rev. D **98**, 114505 \(2018\)](#).
 - [19] S. Rostami, K. Azizi, and A. R. Olamaei, [\(2020\)](#), [arXiv:2008.12715 \[hep-ph\]](#).
 - [20] T. M. Aliev and K. Şimşek, [\(2020\)](#), [arXiv:2011.07150 \[hep-ph\]](#).

- [21] T. M. Aliev and K. Şimşek, [Eur. Phys. J. C](#) **80**, 976 (2020).
- [22] H. I. Alrebdi, T. M. Aliev, and K. Şimşek, [Phys. Rev. D](#) **102**, 074007 (2020).
- [23] K. Azizi, A. R. Olamaei, and S. Rostami, (2020), [arXiv:2011.02919 \[hep-ph\]](#).
- [24] H. F. Jones and M. D. Scadron, [Ann. Phys.](#) **81**, 1 (1973).
- [25] Z. S. Brown, W. Detmold, S. Meinel, and K. Orginos, [Phys. Rev. D](#) **90**, 094507 (2014).
- [26] H. H. Patel, [Comput. Phys. Commun.](#) **197**, 276 (2015).
- [27] T. M. Aliev, K. Azizi, and M. Savcı, [J. Phys. G](#) **40**, 065003 (2013).
- [28] T. M. Aliev, K. Azizi, and M. Savcı, [Nucl. Phys.](#) **A895**, 59 (2012).
- [29] P. Ball, V. M. Braun, Y. Koike, and K. Tanaka, [Nucl. Phys.](#) **B529**, 323 (1998).
- [30] P. Ball and V. Braun, [Nucl. Phys.](#) **B543**, 201 (1999).
- [31] P. Ball and V. M. Braun, [Phys. Rev. D](#) **54**, 2182 (1996).
- [32] P. Ball, V. M. Braun, and A. Lenz, [J. High Energy Phys.](#) **2006**, 004 (2006).
- [33] P. Ball, [J. High Energy Phys.](#) **01**, 010 (1999).
- [34] P. Ball and R. Zwicky, [Phys. Rev. D](#) **71**, 014015 (2005).
- [35] Q. F. Lü, K. L. Wang, L. Y. Xiao, and X. H. Zhong, [Phys. Rev. D](#) **96**, 114006 (2017).
- [36] A. Bernotas and V. Šimonis, [Phys. Rev. D](#) **87**, 074016 (2013).
- [37] R. H. Hackman, N. G. Deshpande, D. A. Dicus, and V. L. Teplitz, [Phys. Rev. D](#) **18**, 2537 (1978).
- [38] T. Branz, A. Faessler, T. Gutsche, M. A. Ivanov, J. G. Körner, V. E. Lyubovitskij, and B. Oehl, [Phys. Rev. D](#) **81**, 114036 (2010).
- [39] E. L. Cui, H. X. Chen, W. Chen, X. Liu, and S. L. Zhu, [Phys. Rev. D](#) **97**, 034018 (2018).